Original Paper

Multi-task learning for seismic elastic parameter inversion with the lateral constraint of angle-gather difference

Pu Wang [a, b, c], Yi-An Cui [a, b, c], Lin Zhou [d], Jing-Ye Li [e], Xin-Peng Pan [a, b, c], Ya Sun [a, b, c, *], Jian-Xin Liu [a, b, c]

[a] Key Laboratory of Metallogenic Prediction of Nonferrous Metals and Geological Environment Monitoring (Central South University), Ministry of Education, Changsha, 410083, Hunan, China
[b] Hunan Key Laboratory of Nonferrous Resources and Geological Hazards Exploration, Changsha, 410083, Hunan, China
[c] School of Geosciences and Info-Physics, Central South University, Changsha, 410083, Hunan, China
[d] School of Earth Sciences and Spatial Information Engineering, Hunan University of Science and Technology, Xiangtan, 411201, Hunan, China
[e] College of Geophysics, China University of Petroleum (Beijing), Beijing, 102249, China

ARTICLE INFO

ABSTRACT

Pre-stack seismic inversion is an effective way to investigate the characteristics of hydrocarbon-bearing reservoirs. Multi-parameter application is the key to identifying reservoir lithology and fluid in pre-stack inversion. However, multi-parameter inversion may bring coupling effects on the parameters and destabilize the inversion. In addition, the lateral recognition accuracy of geological structures receives great attention. To address these challenges, a multi-task learning network considering the angle-gather difference is proposed in this work. The deep learning network is usually assumed as a black box and it is unclear what it can learn. However, the introduction of angle-gather difference can force the deep learning network to focus on the lateral differences, thus improving the lateral accuracy of the prediction profile. The proposed deep learning network includes input and output blocks. First, angle gathers and the angle-gather difference are fed into two separate input blocks with ResNet architecture and Unet architecture, respectively. Then, three elastic parameters, including P- and S-wave velocities and density, are simultaneously predicted based on the idea of multi-task learning by using three separate output blocks with the same convolutional network layers. Experimental and field data tests demonstrate the effectiveness of the proposed method in improving the prediction accuracy of seismic elastic parameters.
© 2024 The Authors. Publishing services by Elsevier B.V. on behalf of KeAi Communications Co. Ltd. This is an open access article under the CC BY-NC-ND license (http://creativecommons.org/licenses/by-nc-nd/4.0/).

1. Introduction

Seismic data is a comprehensive response to the subsurface reservoir characteristics (Mora, 1987; Zong et al., 2015). Seismic inversion is commonly used in hydrocarbon-bearing reservoir exploration (Zhou et al., 2017; Wang et al., 2022). For example, for post-stack seismic inversion, P-wave impedance is predicted to describe the subsurface geological structure, and for pre-stack seismic inversion, P- and S-wave velocities and density are obtained, which are mostly adopted for lithology identification and fluid discrimination (Russell et al., 2003; Kolbjørnsen et al., 2020).

Thus, the study of seismic data is essential for exploring subsurface reservoirs. Seismic angle gathers show the seismic amplitude versus incident angle (AVA). The AVA characteristics vary depending on the elastic parameters of the subsurface reservoir. The elastic parameters are determined by the petrophysical properties (Zhao et al., 2021; Pan et al., 2022). Thus, different AVA patterns correspond to different hydrocarbon-bearing properties, which is the theoretical basis for the AVA simulation and inversion. Compared with post-stack seismic inversion, AVA inversion can predict multiple parameters, thus providing more detailed reservoir information (Zong et al., 2018; Yuan et al., 2018). However, angle gathers show the AVA characteristics of a single trace and the AVA inversion is usually a trace-by-trace inversion, which may cause lateral discontinuity of inversion results and limit the lateral identification accuracy of subsurface geological structure. To highlight the lateral difference, Wang et al. (2020a) introduced the angle-gather

---

* Corresponding author. School of Geosciences and Info-Physics, Central South University, Changsha, 410083, Hunan, China.
E-mail address: sunya_seis@csu.edu.cn (Y. Sun).

difference and proposed a seismic AVA inversion method constrained by the angle-gather difference. For AVA inversion, the coupling relationship between elastic parameters is also a highly noteworthy problem (Zhi et al., 2016). Besides, the seismic wave propagation theories, such as Zoeppritz's equation, are usually nonlinear, which brings challenges to seismic inversion (Guo et al., 2021). Thus, for high-precise reservoir prediction, the conventional AVA inversion has limitations.

In recent years, a variety of machine learning approaches are applied to geophysical exploration and reservoir prediction (Chai et al., 2020; Yu and Ma, 2021; Li et al., 2023). For example, Markov chain Monte Carlo methods are used to evaluate the reliability of the results by posterior probabilities (Grana, 2016; Conjard and Grana, 2021), the Hidden Markov model is used to extract the hidden properties to improve the prediction (Feng et al., 2018; Wang et al., 2020b), and the random forest method is used for classification and regression problems in reservoir studies (Ao et al., 2020). Among them, the deep learning approaches are of great interest. They are widely adopted for fault interpretation (Wu et al., 2019), geological structure identification (Gao et al., 2021), lithology discrimination (Zhang et al., 2018), etc. Deep learning approaches have a strong nonlinear mapping ability. It can fully exploit the information underlying the data, which helps to describe the relationship between seismic data and reservoir parameters (Li et al., 2022). To handle the problems of AVA inversion mentioned above, a multi-task learning network considering the angle-gather difference is proposed in this paper. Since deep learning approaches are data-driven methods, the diversity of the training data has a significant impact on prediction accuracy. The deep learning network is often considered to be a black box, and it is difficult to capture the focus of training and the ability of learning. In this paper, the interpretability of the network is increased by expanding the input data. To highlight the lateral difference, the angle-gather difference is used, and they serve as input data together with angle gathers. By using this approach, the deep learning network is forced to learn lateral variation characteristics. Thus, it is possible to understand what a deep learning network has learned by changing or increasing the types of input data. This can enhance the physical meaning of deep learning approaches. In addition, to weaken the coupling relationship between elastic parameters, the idea of multi-task learning is adopted. Multi-task learning configures different output blocks for different tasks, and they are trained to obtain their respective optimization parameters. The total loss function is obtained by summing the contributions of the loss functions of each task. In the deep learning network architecture, the shared network part is for extracting commonalities, while the separate network part is for extracting differences. Thus, multi-task learning can be adopted to improve the prediction accuracy of the multi-parameter inversion based on AVA data.

In this paper, the angle-gather difference is first analyzed. Then, the construction of the multi-task learning network considering the angle-gather difference is introduced in detail. Finally, the experimental and field data tests are presented.

2. Theory

In this section, the difference angle gathers are analyzed to illustrate their ability to reveal lateral differences, and a multi-task learning network considering difference angle gathers is constructed.

2.1. Angle-gather difference analysis

According to Wang et al. (2020a), the angle-gather difference represents the difference of angle gathers between different traces. Thus, they can be used to depict the lateral variation of reservoir parameters. In this paper, we first set the reference trace, and then constrain the seismic parameter prediction by considering the differences between the reference trace and the other traces. The angle-gather difference is expressed as

$$\Delta \mathbf{d} = \mathbf{d}_i - \mathbf{d}_{\text{ref}} \tag{1}$$

where $\Delta \mathbf{d}$ refers to the matrix consisting of angle-gather difference. $\mathbf{d}$ is the matrix of angle gathers. The subscript i indicates the i-th trace and ref indicates the reference trace. For the field data, the reference trace can be set to the well-side trace.

A set of synthetic data is applied to analyze the angle-gather difference. The 1500th trace is set as the reference trace. Fig. 1 shows the P-wave velocity profile of the Marmousi2 model. The synthetic angle gathers shown in Fig. 2(a) and (c) are obtained using the P- and S-wave velocities and density at traces 1500 and 1000. The forward modeling operator is the convolution of reflection coefficient and the Ricker wavelet:

$$\mathbf{G}(\boldsymbol{m}_i) = R_{\text{PP}}(\boldsymbol{m}_i) * W \tag{2}$$

where $\mathbf{G}(\bullet)$ refers to the forward modeling operator. The main frequency of the Ricker wavelet W is about 35 Hz. $\boldsymbol{m}$ indicates the elastic parameters, including P- and S-wave velocities and density. $R_{\text{PP}}(\boldsymbol{m}_i)$ refers to the reflection coefficient by using Zoeppritz's equation. Based on the matrix by Aki and Richards (1980), the P-wave reflection coefficient is explicitly given as follows:

$$R_{\text{PP}} = \frac{\left[\left(b \frac{\cos \theta_1}{V_{P1}} - c \frac{\cos \theta_2}{V_{P2}} \right) F - \left(a + d \frac{\cos \theta_1}{V_{P1}} \frac{\cos \varphi_2}{V_{S2}} \right) Hp^2 \right]}{D} \tag{3}$$

where

$$a = \rho_2 \left(1 - 2 \sin^2 \varphi_2 \right) - \rho_1 \left(1 - 2 \sin^2 \varphi_1 \right)$$

$$b = \rho_2 \left(1 - 2 \sin^2 \varphi_2 \right) + 2 \rho_1 \sin^2 \varphi_1$$

$$c = \rho_1 \left(1 - 2 \sin^2 \varphi_1 \right) + 2 \rho_2 \sin^2 \varphi_2$$
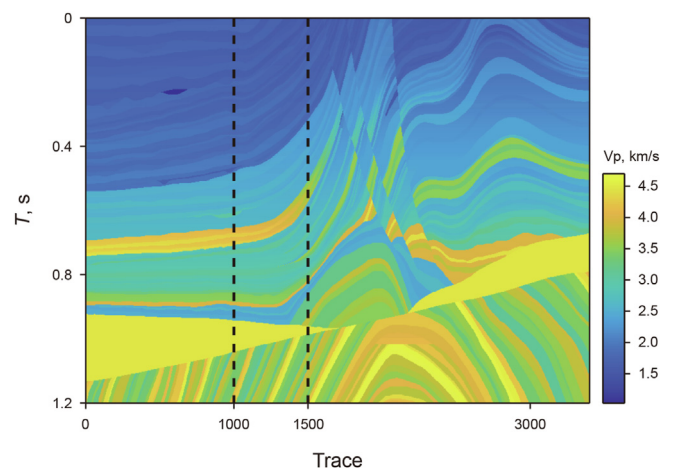

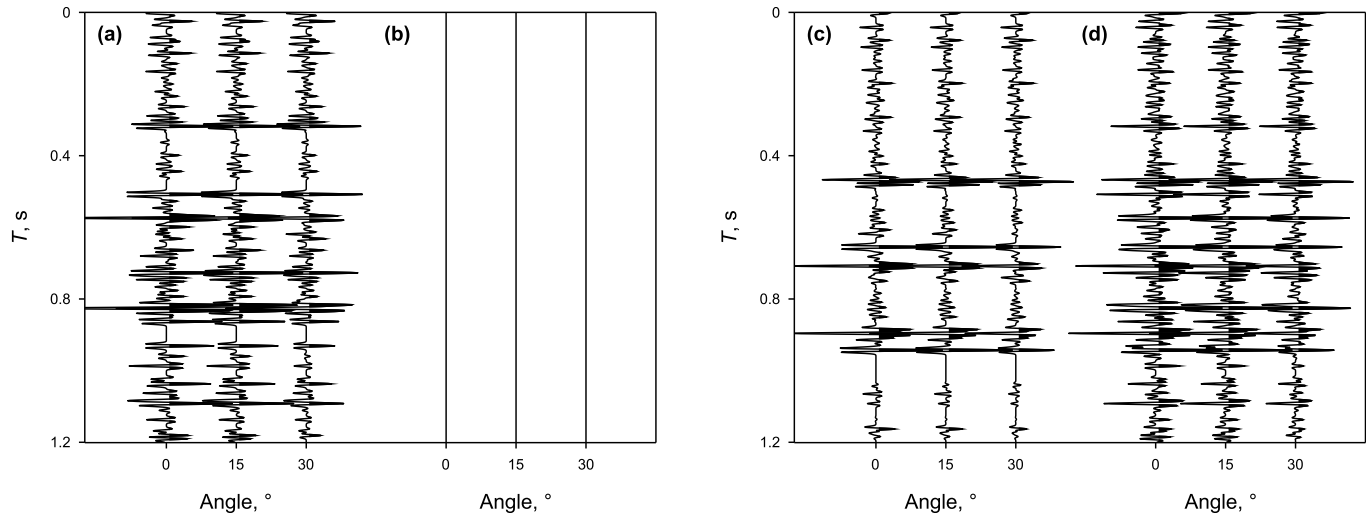**Fig. 1.** P-wave velocity (Vp) profile of the Marmousi2 model.

Fig. 2. (a) and (c) are the seismic angle gathers at traces 1500 and 1000, (b) and (d) are the angle-gather difference between trace 1500 and itself and the angle-gather difference between traces 1000 and 1500.

$$d = 2\left(\rho_2 V_{S2}^2 - \rho_1 V_{S1}^2\right)$$

$$D = EF + GHp^2$$

$$E = b\frac{\cos\theta_1}{V_{P1}} + c\frac{\cos\theta_2}{V_{P2}}$$

$$F = b\frac{\cos\varphi_1}{V_{S1}} + c\frac{\cos\varphi_2}{V_{S2}}$$

$$G = a - d\frac{\cos\theta_1}{V_{P1}}\frac{\cos\varphi_2}{V_{S2}}$$

and

$$H = a - d\frac{\cos\theta_2}{V_{P2}}\frac{\cos\varphi_1}{V_{S1}}$$

where θ_1, θ_2, φ_1 and φ_2 are the incident and transmitted angle of P-wave, the reflected and transmitted angle of S-wave respectively; ρ_1, V_{P1} and V_{S1} are the density, the velocity of P-wave and the velocity of S-wave of the upper layer; ρ_2, V_{P2} and V_{S2} are the density, the velocity of P-wave and the velocity of S-wave of the lower layer; p is the ray parameter.

For synthetic data, Eq. (1) is re-expressed by using the following equation based on the forward modeling theory:

$$\Delta \mathbf{G}(\mathbf{m}_i) = \mathbf{G}(\mathbf{m}_i) - \mathbf{G}\left(\mathbf{m}_{\text{ref}}\right) \tag{4}$$

According to the study of Wang et al. (2020a), the difference of angle gathers can be used to improve the elastic parameter prediction by using the Bayesian inversion framework. In this work, we investigate the improvement of lateral accuracy by proposing a new deep network. It should be pointed out that increasing lateral accuracy means not only the improvement of lateral connectivity, but also a clearer delineation of the lateral boundaries of the subsurface geologic bodies.

Fig. 2(b) shows the angle-gather difference at the reference trace obtained by subtracting the angle gathers of the reference trace from themselves, and they are all zero. This is a limit case, representing no differences in the lateral direction. Fig. 2(d) shows the angle-gather difference between traces 1000 and 1500. Similar to the angle gathers, the angle-gather difference also varies with the incident angle. They are sensitive to subsurface formations with lateral variations and large differences between the upper and lower layers. Thus, the introduction of angle-gather difference helps to explore the hidden relationship between seismic data and elastic parameters.

From Fig. 2(a) and (c), the angle gathers represent the vertical differences of the elastic parameters at traces 1500 and 1000. Since the deep learning network is a black box, it is not clear from the user's perspective whether the deep learning network can capture the lateral difference between them if only angle gathers are used. Thus, the angle-gather difference shown in Fig. 2(b) and (d) can be used to expand the input data, which allows for better learning of lateral differences. This helps to depict the lateral boundaries of subsurface geological bodies with high accuracy.

2.2. Network architecture of multi-task learning considering angle-gather difference

In pre-stack seismic inversion, the seismic data generally refers to angle gathers only. To improve the lateral prediction accuracy, the angle-gather difference is used to expand the input data. First, angle gathers and the angle-gather difference are fed into two separate input blocks, Input Block 1 and Input Block 2, in Fig. 3. Deep networks are widely used to uncover the intrinsic relationships between different sets of data. However, the complexity of these relationships is uncertain. Therefore, excessive network layers may cause overfitting and thus local minima, as well as degradation problems and convergence slowdowns. Residual networks (ResNets) are alternative methods to ensure the convergence and accuracy of multilayer networks (Wu et al., 2020). Skip connections are the key to deep ResNets, which allow simple network blocks or direct connections to weaken the degradation problem. In this paper, we build a new deep network as shown in Fig. 3, where the ResNet architecture given in Fig. 4 is used as the input block for the angle gathers. From Fig. 4, a simple convolutional layer (sub-block B) is taken as the skip connection to avoid the gradient vanishing due to using multiple sets of sub-block A. In addition, another block, the Unet architecture given in Fig. 5, is used as the input block for the angle-gather difference, where the skip
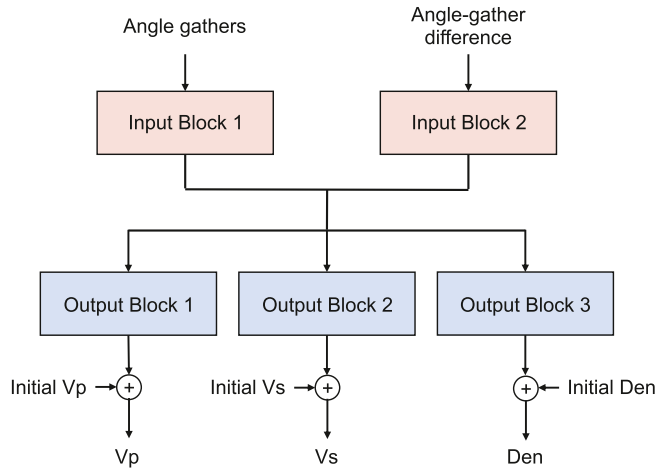
Fig. 3. The deep learning network architecture for multi-parameter seismic prediction with two input blocks. Vp, Vs and Den indicate P- and S-wave velocities and density, respectively; Initial Vp, Initial Vs and Initial Den are low-frequency initial models of P- and S-wave velocities and density.
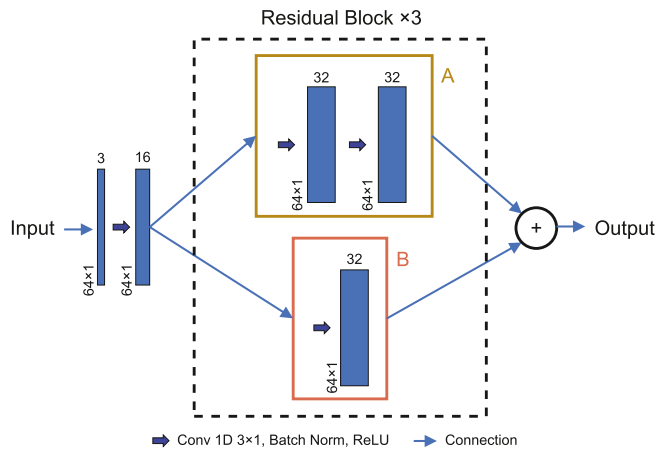

Fig. 4. The network architecture and network parameters of Input Block 1. Before feeding data, the input data length is extended from 3 to 64.

connection is implemented by copying and cropping, which can preserve large-scale features coming from the upper layers, thus highlighting lateral structural variations and maintaining lateral continuity. In this work, the ResNet and Unet architectures are adopted to learn the vertical details and horizontal geologic
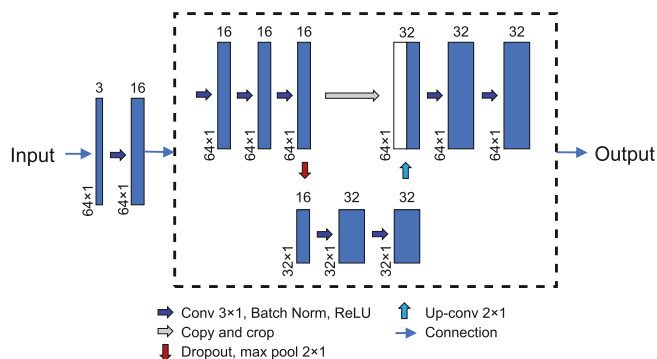

Fig. 5. The network architecture and network parameters of Input Block 2. Before feeding data, the input data length is extended from 3 to 64.
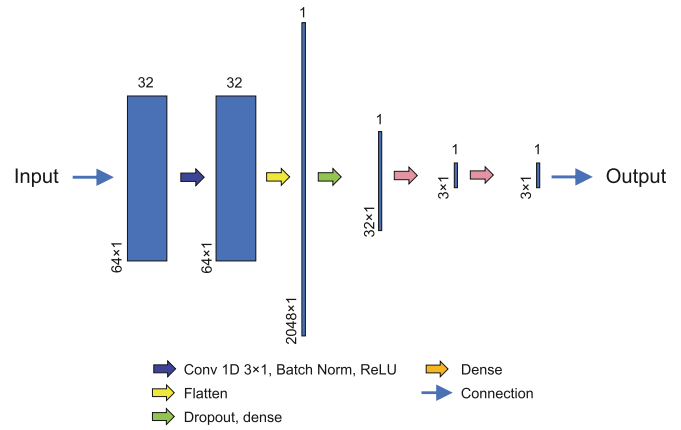

Fig. 6. The network architecture and network parameters of Output Blocks 1, 2, and 3. The output data length is 3.
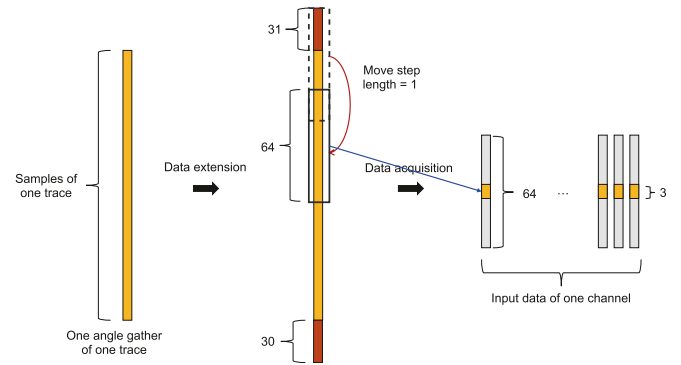

Fig. 7. Expansion process of input data.

structural variations separately.

Then, the outputs of these two input blocks are fused and passed to three separate output blocks to accomplish the multitask learning of P- and S-wave velocities and density. The output block is shown in Fig. 6, which includes several convolutional layers and dense layers. By combining Figs. 3–6, the final network architecture is built. The network parameters are given in Figs. 4–6. They are adjusted following the arguments of Wu et al. (2020) and Meng et al. (2021). In this work, the input data is set longer than the output data in order to account for the wavelet effect. To consider the influence of wavelet, the input data are extended. This is
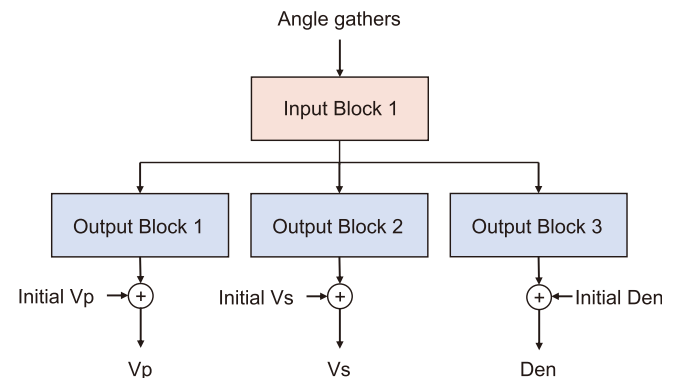

Fig. 8. The deep learning network architecture for multi-parameter seismic prediction with one input block.
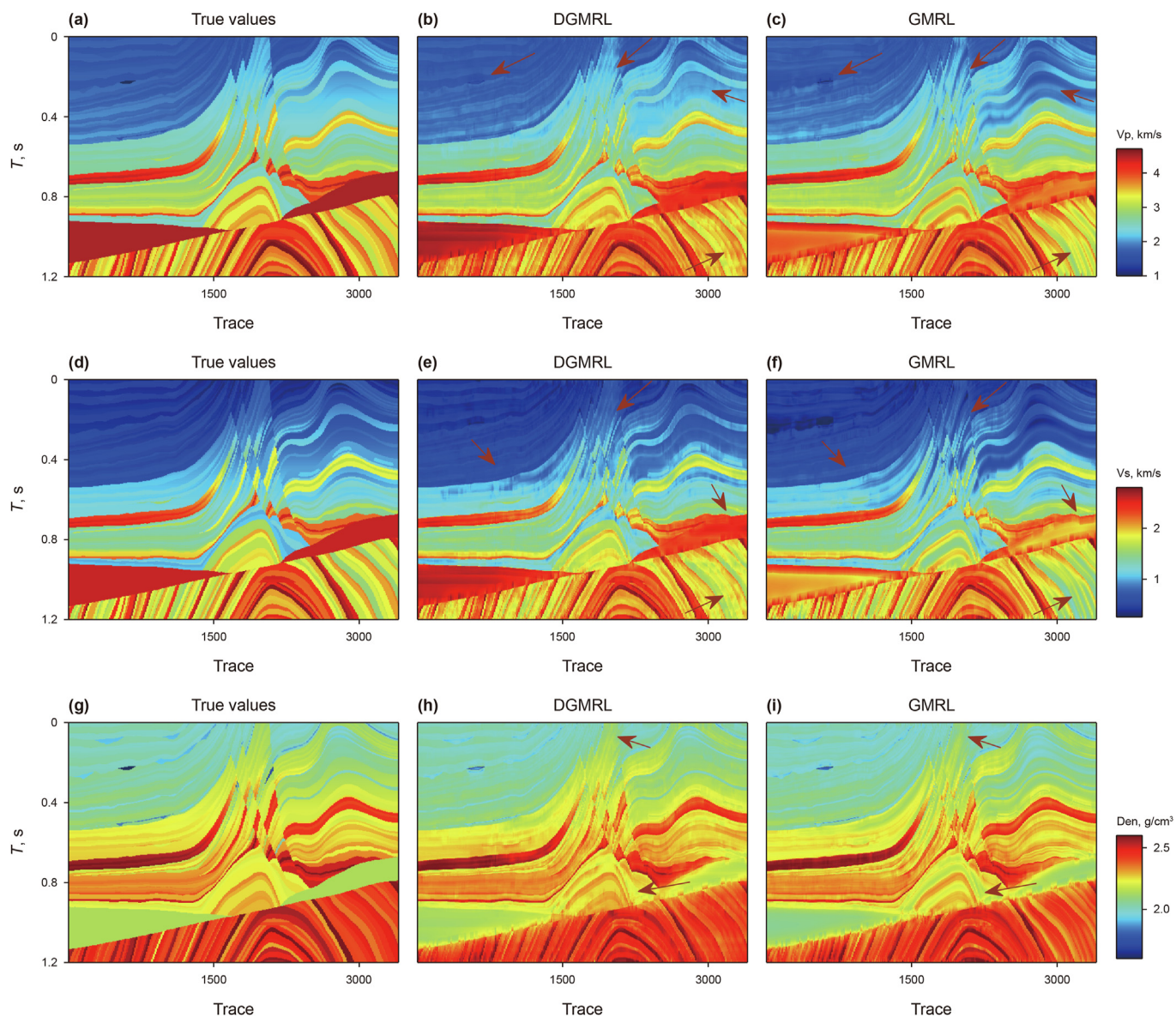
Fig. 9. Predicted elastic parameter profiles by using the DGMRL and GMRL approaches. **(a)**, **(d)** and **(g)** are the true elastic parameters of the Marmousi2 model; **(b)**, **(e)** and **(h)** are the predicted elastic parameters by using the DGMRL approach; **(c)**, **(f)** and **(i)** are the predicted elastic parameters by using the GMRL approach.

because that the wavelet has a certain length in time. The output data length is set to 3 and the input data length is extended from 3 to 64 by using proximity points (Fig. 7). Each sample in a channel is generated by setting the window length to 64 and the move step to 1. Different channels are fed with different angles.

The deep learning of angle gathers helps to depict the vertical variation of reservoir parameters, while the deep learning of angle-gather difference helps to reveal the lateral variation. Thus, they are considered to be combined in this paper. To highlight the differences between these two sets of data, they are fed into separate input blocks. In addition, the multi-task learning idea is adopted to weaken the multi-parameter coupling. The loss function follows that the sum of the mean square errors of different outputs is minimum. The parameters in the network are optimized by using the Adam algorithm. To improve the nonlinearity of the deep network, the rectified linear unit (ReLU) is used. To prevent the deep network from overfitting, the dropout layer is adopted in output blocks.

3. Application

In this section, two sets of synthetic data are first used to test the proposed deep network. The angle gathers are generated by using the Ricker wavelet with the main frequency of 35 Hz and the elastic parameters of the Marmousi2 and Overthrust models. The angle ranges from 0° to 30° with an interval of 15°. Then, the proposed approach is tested by using the field data from a work area in Eastern China. The effective angle range is $3°-45°$.

In our study, only several wells are used to analyze the prediction effects using small sample sets. The Marmousi2 model is trained with a sample set of four traces, 200, 800, 2000 and 3000. For the Overthrust model, two traces, 300 and 600, are used for training. These extracted traces are regarded as pseudo-wells. To reveal the lateral variation, the 800th trace of the Marmousi2 model is considered as the reference trace, and for the Overthrust model, the reference trace is the 600th trace. The reference trace can be specified arbitrarily, with the premise that the angle-gather
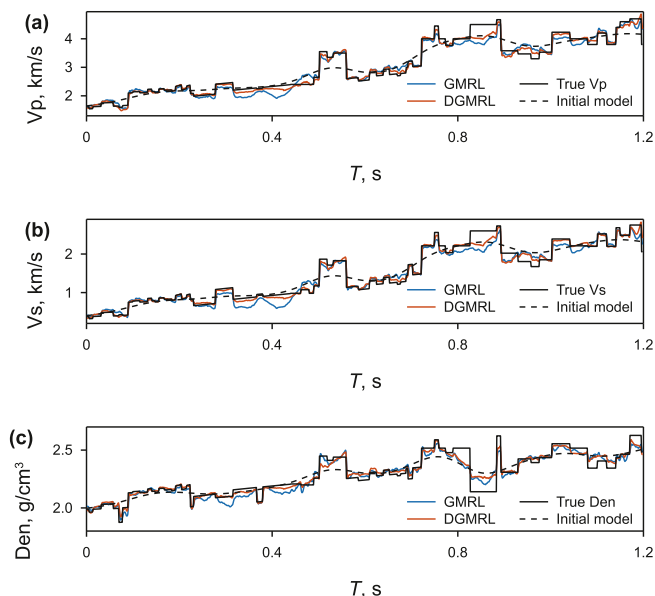
Fig. 10. Predicted elastic parameter curves by using the DGMRL and GMRL approaches at trace 2500. The initial model is the low-frequency model.

difference between the reference trace and itself as shown in Fig. 2(b) must be trained. Then the angle-gather difference between other traces and the reference trace are fed into the proposed deep learning network. When angle gathers and the angle-gather difference are input, different angles are assigned to different channels, where three channels are assigned.

We compare the proposed approach in Fig. 3 with the deep network architecture without considering the angle-gather difference as shown in Fig. 8. Here, the proposed approach is named DGMRL (difference angle gather constrained multi-task residual deep learning approach), and the approach shown in Fig. 8 is named GMRL (angle gather-based multi-task residual deep learning approach).

We first test our approach on the Marmousi2 model. The total number of training sets is 4800. With GPU acceleration, the training time for 1000 iterations is about 600 s. Fig. 9 shows the predicted
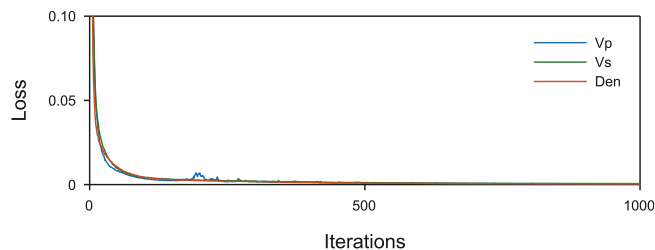

Fig. 12. Changes in the loss functions of different parameters during training. Vp, Vs and Den indicate P- and S-wave velocities and density, respectively.

elastic parameter profiles by using the DGMR and GMRL approaches. By comparison, the vertical resolution of the elastic parameters in Fig. 9(b), (e) and (h) is higher and the lateral continuity is better due to the consideration of the angle-gather difference, especially for the areas indicated by the red arrows. In addition, more lateral details are presented with the proposed approach and the underground anomalies are described more clearly compared with the GMRL approach. To better highlight the superiority of the proposed approach, the P- and S-wave velocities and density at trace 2500 are extracted and their curves are compared in Fig. 10. It is observed that the results obtained by the proposed approach are closer to the underground truth, and they are more stable and less fluctuating than those by using the GMRL approach. In this work, low-frequency model is used as the initial model to improve the results. The initial model helps to avoid the solution falling into a local minimum. Fig. 11 shows the relative errors of P-wave velocities by using the DGMRL approach and the GMRL approach. It can be seen that the relative error of the proposed approach (Fig. 11(a)) is smaller and is more concentrated within 5%. The changes in the loss functions for multitask training are shown in Fig. 12, which indicates the proposed approach has a good convergence rate. For ResNets, the skip connection allows the residual network to converge efficiently but may bring fluctuations in the results. The incorporation of several sets of residual blocks in Fig. 4 enables the deep learning network to focus on more details, which can weaken the fluctuation of prediction results. However, this enhancement is not sufficient in terms of the prediction results of the GMRL method. In this work, the introduction of angle-gather difference can provide more reservoir details, and the Unet architecture in
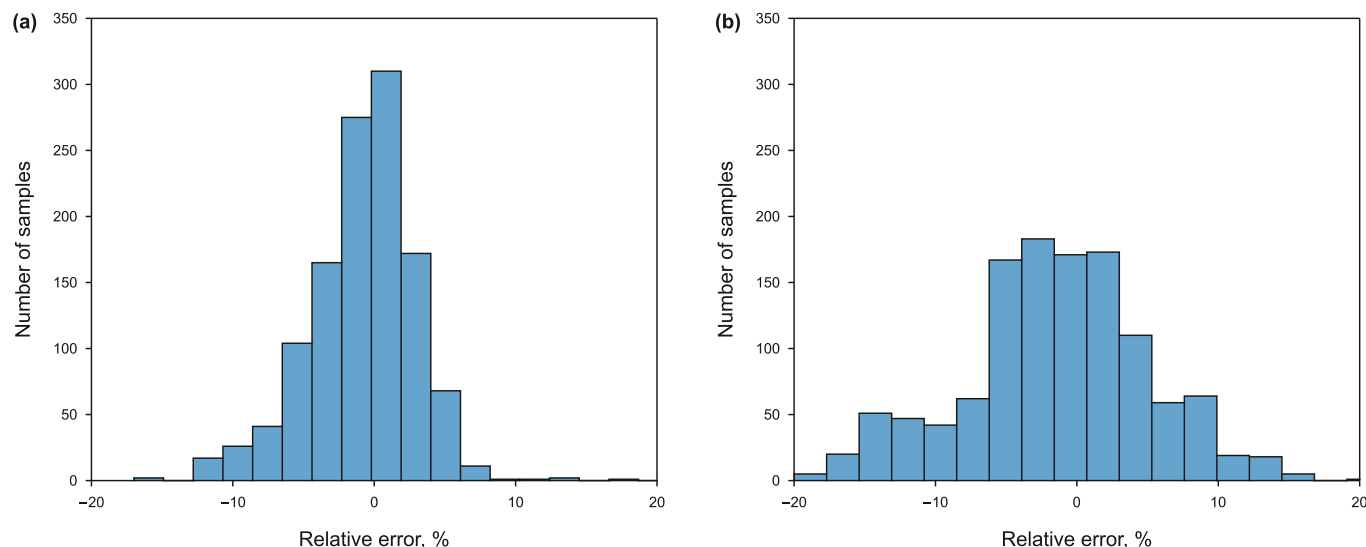

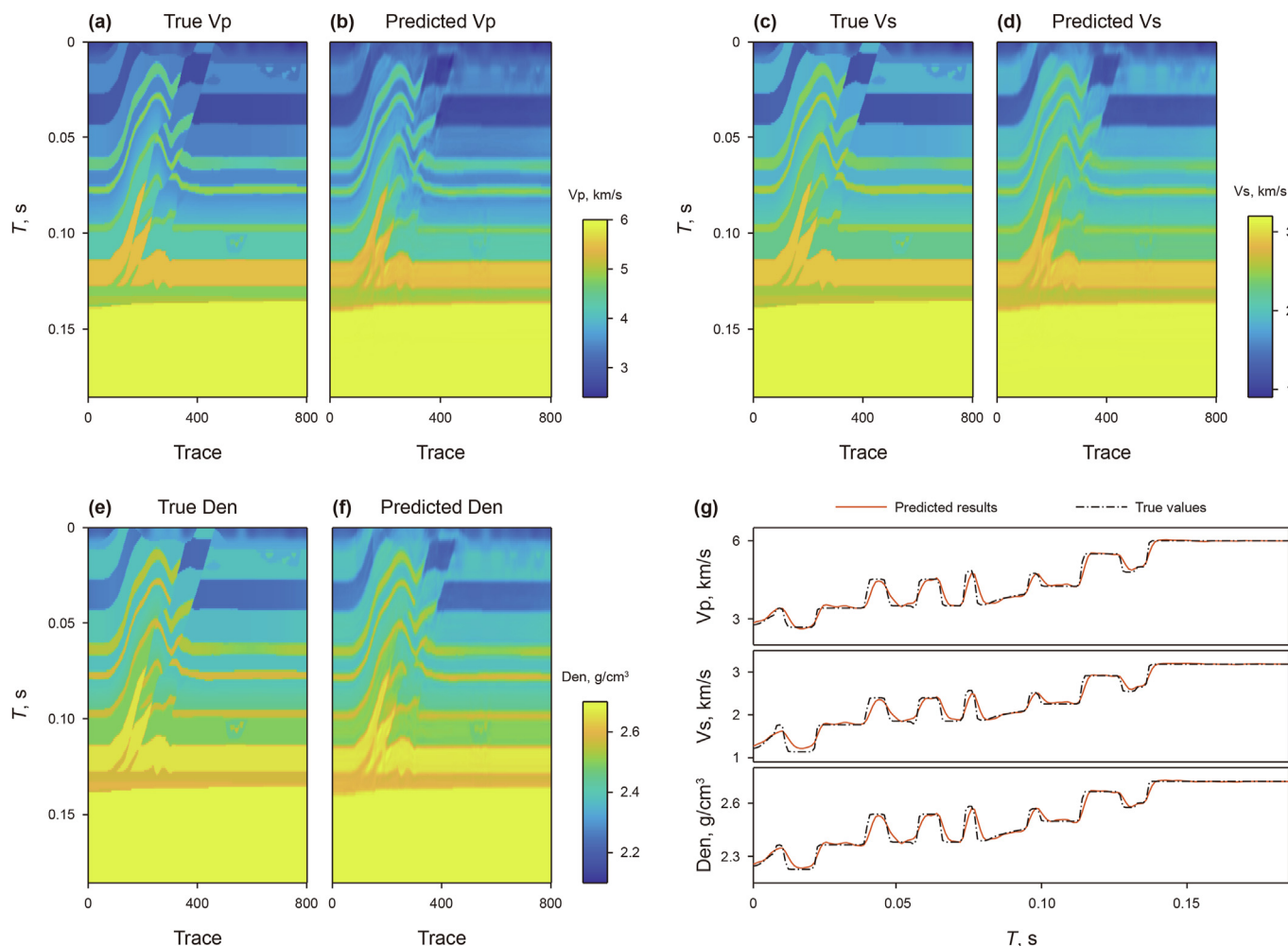**Fig. 11.** Relative errors of P-wave velocities at trace 2500 by using the DGMRL approach (**a**) and the GMRL approach (**b**).

Fig. 13. Predicted elastic parameter profiles and curves by using the proposed DGMRL approach for the Overthrust model. (**a**), (**c**) and (**e**) are the true elastic parameters of the Overthrust model; (**b**), (**d**) and (**f**) are the predicted elastic parameters by using the DGMRL approach; (**g**) is the predicted curves of elastic parameters at trace 350.

Fig. 5 brings large-scale attributes that help to weaken the lateral discontinuities caused by the commonly used trace-by-trace inversion, thus improving the prediction accuracy and stability. Thus, both lateral and vertical details are highlighted by using the proposed approach.

We then test our approach on the Overthrust model. Since the geological structure of this model is not as complex as that of the Marmousi2 model, the accuracy of the predicted results may be higher. Here, only the proposed method is applied and its validity is illustrated by comparison with the true values. The predicted profiles of elastic parameters by using the DGMRL approach are given in Fig. 13(b) and (d) and (f), and the curve comparisons at trace 350 are shown in Fig. 13(g). It can be seen that the predicted results by using the proposed approach match well with the true values.

We also test our approach on the field data. The stack profile of the angle gathers is shown in Fig. 14(h). Only two wells are used here, one of which is treated as the reference trace. For the field data, the seismic data at well-side trace is used as the training sample set. The initial models are also used here, which are low-frequency models obtained through logging and horizon interpretation. Fig. 14(a), (c) and (e) show the profiles of P- and S-wave velocities and density by using the GMRL approach. The predicted profiles of elastic parameters by using the DGMRL approach are given in Fig. 14(b) and (d) and (f), and the curve comparisons at CDP 41 are displayed in Fig. 14(g). The comparison of predicted profiles

shows that the proposed approach can obtain more details of the reservoir. Both vertical and horizontal resolutions are improved. From Fig. 14(b), (d) and (f), the inclined events indicated by the red arrows are maintained and become more continuous. The areas indicated by the black arrows have more horizontal detail and can highlight small elastic changes, which helps to distinguish small geologic anomalies. From Fig. 14(g), it can be seen that the predicted results by using the proposed approach match better with the well-logging curves. As in the previous analysis, the same conclusion can be drawn that the introduction of angle-gather difference can assist seismic inversion to yield high-precise elastic parameters, which is crucial for the fine description of reservoirs, as well as for lithology identification and fluid discrimination. Note that enhancing lateral accuracy does not only refer to improving lateral continuity, but also to highlighting the lateral contact relationships of subsurface anomalies. From Fig. 14(b), (d) and (f), the large events are still maintained and more lateral details are present.

From the above three tests, it can be seen that the proposed multi-task learning network using residual blocks and Unet block, and considering the angle-gather difference helps to improve the prediction accuracy of seismic elastic parameters. In our further study, noise suppression will be considered by feeding different noises into the network.
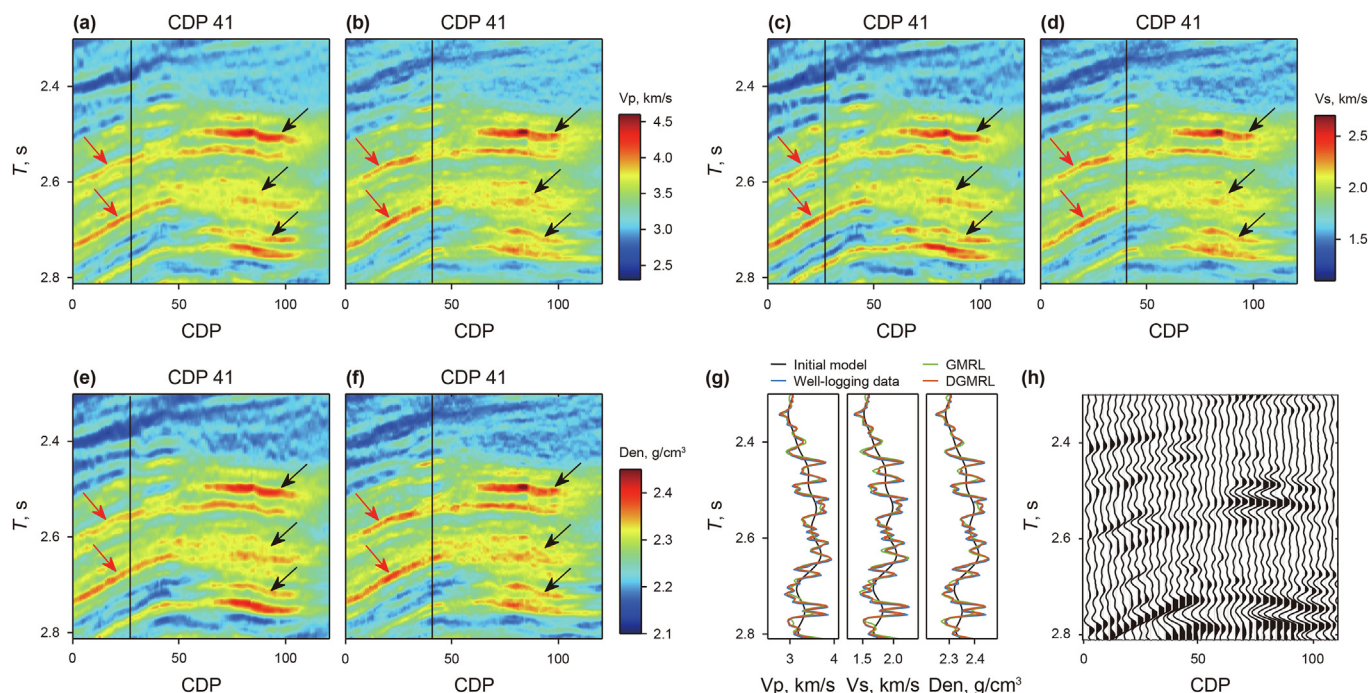
Fig. 14. Predicted elastic parameter profiles and curves by using the GMRL approach and the proposed DGMRL approach. **(a)**, **(c)** and **(e)** are the predicted elastic parameters by using the GMRL approach; **(b)**, **(d)** and **(f)** are the predicted elastic parameters by using the DGMRL approach; **(g)** shows the predicted and well-logging curves of elastic parameters at CDP 41; **(h)** is the stack profile of the angle gathers.

4. Conclusion

Reservoir parameter prediction is the key to seismic exploration. However, the pre-stack AVA inversion is usually a trace-by-trace inversion, which may cause lateral discontinuities. To address this problem, we propose a multi-task deep learning network by considering the angle-gather difference. The network architecture contains two separate input blocks for vertical and lateral constraints by inputting angle gathers and angle-gather difference, and three output blocks for multi-parameter prediction of P- and S-wave velocities and density. The input blocks have two different compositions, the ResNet architecture and the Unet architecture, which help to ensure convergence and prediction accuracy. The output blocks can effectively avoid the coupling between multiple parameters. The introduction of angle-gather difference can increase the interpretability of deep learning by forcing the network to learn lateral characteristics, which is a key point of the paper. Experimental and field data tests demonstrate the feasibility of our approach.

Declaration of interests

The authors declare that they have no known competing financial interests or personal relationships that could have appeared to influence the work reported in this paper.

CRediT authorship contribution statement

Pu Wang: Writing − original draft, Methodology. **Yi-An Cui:** Validation. **Lin Zhou:** Investigation. **Jing-Ye Li:** Data curation. **Xin-Peng Pan:** Methodology. **Ya Sun:** Writing − original draft. **Jian-Xin Liu:** Funding acquisition.

References

Aki, K., Richards, P.G., 1980. Quantitative Seismology: Theory and Methods. W. H. Freeman and Co, San Francisco, CA.

Ao, Y., Lu, W., Hou, Q., Jiang, B., 2020. Synthesize nuclear magnetic resonance T2 spectrum from conventional logging responses with spectrum regression forest. Geosci. Rem. Sens. Lett. IEEE 18 (10), 1726−1730. https://doi.org/10.1109/LGRS.2020.3008183.

Chai, X., Tang, G., Wang, S., Lin, K., Peng, R., 2020. Deep learning for irregularly and regularly missing 3-D data reconstruction. IEEE Trans. Geosci. Rem. Sens. 59 (7), 6244−6265. https://doi.org/10.1109/TGRS.2020.3016343.

Conjard, M., Grana, D., 2021. Ensemble-based seismic and production data assimilation using selection Kalman model. Math. Geosci. 53 (7), 1445−1468. https://doi.org/10.1007/s11004-021-09940-2.

Feng, R., Luthi, S.M., Gisolf, D., Angerer, E., 2018. Reservoir lithology classification based on seismic inversion results by hidden Markov models: applying prior geological information. Mar. Petrol. Geol. 93, 218−229. https://doi.org/10.1016/j.marpetgeo.2018.03.004.

Gao, H., Wu, X., Liu, G., 2021. ChannelSeg3D: channel simulation and deep learning for channel interpretation in 3D seismic images. Geophysics 86 (4), IM73−IM83. https://doi.org/10.1190/GEO2020-0572.1.

Grana, D., 2016. Bayesian linearized rock-physics inversion. Geophysics 81 (6), D625−D641. https://doi.org/10.1190/GEO2017-0463.1.

Guo, Q., Ba, J., Fu, L.Y., Luo, C., 2021. Joint seismic and petrophysical nonlinear inversion with Gaussian mixture-based adaptive regularization. Geophysics 86 (6), R895−R911. https://doi.org/10.1190/GEO2021-0017.1.

Kolbjørnsen, O., Buland, A., Hauge, R., Røe, P., Ndingwan, A.O., Aker, E., 2020. Bayesian seismic inversion for stratigraphic horizon, lithology, and fluid prediction. Geophysics 85 (3), R207−R221. https://doi.org/10.1190/GEO2019-0170.1.

Li, D., Peng, S., Guo, Y., Lu, Y., Cui, X., Du, W., 2022. Progressive multitask learning for high-resolution prediction of reservoir elastic parameters. Geophysics 88 (2), M71−M86. https://doi.org/10.1190/GEO2022-0275.1.

Li, D., Guo, Y., Peng, S., Li, C., Lin, P., 2023. Time-lapse seismic matching for CO2 plume detection via correlation-based recurrent attention network. IEEE Trans. Geosci. Rem. Sens. 61, 1−10. https://doi.org/10.1109/TGRS.2023.3308966.

Meng, J., Wang, S., Cheng, W., Wang, Z., Yang, L., 2021. AVO inversion based on transfer learning and low-frequency model. Geosci. Rem. Sens. Lett. IEEE 19, 1—5. https://doi.org/10.1109/LGRS.2021.3132426.

Mora, P., 1987. Nonlinear two-dimensional elastic inversion of multioffset seismic data. Geophysics 52 (9), 1211—1228. https://doi.org/10.1190/1.1442384.

Pan, X., Lu, C., Zhang, G., Wang, P., Liu, J., 2022. Seismic characterization of naturally fractured reservoirs with monoclinic symmetry induced by horizontal and tilted fractures from amplitude variation with offset and azimuth. Surv. Geophys. 43 (3), 815—851. https://doi.org/10.1007/s10712-022-09709-0.

Russell, B.H., Hedlin, K., Hilterman, F.J., Lines, L.R., 2003. Fluid-property discrimination with AVO: a Biot-Gassmann perspective. Geophysics 68 (1), 29—39. https://doi.org/10.1190/1.1543192.

Wang, P., Chen, X., Li, J., Wang, B., 2020a. Lateral constrained prestack seismic inversion based on difference angle gathers. Geosci. Rem. Sens. Lett. IEEE 18 (12), 2177—2181. https://doi.org/10.1109/LGRS.2020.3014815.

Wang, P., Chen, X., Wang, B., Li, J., Dai, H., 2020b. An improved method for lithology identification based on a hidden Markov model and random forests. Geophysics 85 (6), IM27—IM36. https://doi.org/10.1190/GEO2020-0108.1.

Wang, P., Cui, Y., Liu, J., 2022. Fluid discrimination based on inclusion-based method for tight sandstone reservoirs. Surv. Geophys. 43 (5), 1469—1496.

Wu, B., Meng, D., Wang, L., Liu, N., Wang, Y., 2020. Seismic impedance inversion using fully convolutional residual network and transfer learning. Geosci. Rem. Sens. Lett. IEEE 17 (12), 2140—2144. https://doi.org/10.1109/LGRS.2019.2963106.

Wu, X., Liang, L., Shi, Y., Geng, Z., Fomel, S., 2019. Multitask learning for local seismic image processing: fault detection, structure-oriented smoothing with edge-preserving, and seismic normal estimation by using a single convolutional neural network. Geophys. J. Int. 219 (3), 2097—2109. https://doi.org/10.1093/gji/ggz418.

Yu, S., Ma, J., 2021. Deep learning for geophysics: Current and future trends. Rev. Geophys. 59 (3), e2021RG000742. https://doi.org/10.1029/2021RG000742.

Yuan, S., Liu, Y., Zhang, Z., Luo, C., Wang, S., 2018. Prestack stochastic frequency-dependent velocity inversion with rock-physics constraints and statistical associated hydrocarbon attributes. Geosci. Rem. Sens. Lett. IEEE 16 (1), 140—144. https://doi.org/10.1109/LGRS.2018.2868831.

Zhang, G., Wang, Z., Chen, Y., 2018. Deep learning for seismic lithology prediction. Geophys. J. Int. 215 (2), 1368—1387. https://doi.org/10.1093/gji/ggy344.

Zhao, L., Wang, Y., Yao, Q., Geng, J., Li, H., Yuan, H., Han, D.H., 2021. Extended Gassmann equation with dynamic volumetric strain: modeling wave dispersion and attenuation of heterogeneous porous rocks. Geophysics 86 (3), MR149—MR164. https://doi.org/10.1190/GEO2020-0395.1.

Zhi, L., Chen, S., Li, X., 2016. Amplitude variation with angle inversion using the exact Zoeppritz equations - theory and methodology. Geophysics 81 (2), N1—N15. https://doi.org/10.1190/GEO2014-0582.1.

Zhou, L., Li, J., Chen, X., Liu, X., Chen, L., 2017. Prestack amplitude versus angle inversion for Young's modulus and Poisson's ratio based on the exact Zoeppritz equations. Geophys. Prospect. 65 (6), 1462—1476. https://doi.org/10.1111/1365-2478.12493.

Zong, Z., Wang, Y., Li, K., Yin, X., 2018. Broadband seismic inversion for low-frequency component of the model parameter. IEEE Trans. Geosci. Rem. Sens. 56 (9), 5177—5184. https://doi.org/10.1109/TGRS.2018.2810845.

Zong, Z., Yin, X., Wu, G., 2015. Geofluid discrimination incorporating poroelasticity and seismic reflection inversion. Surv. Geophys. 36 (5), 659—681. https://doi.org/10.1007/s10712-015-9330-6.